DMD Fast Forward. Published on January 6, 2011 as doi:10.1124/dmd.110.036400
This article has not been copyedited and formatted. The final version may differ from this version.

Prediction of CYP3A Mediated Drug-Drug Interactions Using Human Hepatocytes Suspended in Human Plasma

Jialin Mao, Michael A. Mohutsky, John P. Harrelson, Steven A. Wrighton and Stephen D. Hall

JM, MAM, SAW and SDH: Department of Drug Disposition, Lilly Research Labs, Eli Lilly and Co., Indianapolis, IN; JPH: School of Pharmacy, Pacific University, Hillsboro, OR

Running title: CYP3A DDI Prediction Using Human Hepatocytes in Human Plasma

To whom correspondence should be addressed:

Jialin Mao, Ph.D.

Drug Disposition

Lilly Research Labs, Eli Lilly and Co.

Lilly Corporate Center

Indianapolis, IN, 46285

Phone: 317-433-7896

Fax: 317-433-9287

Email: mao_jialin@lilly.com

The number of text pages: 24

The number of tables: 3

The number of figures: 4

The number of reference: 67

The number of words in the *Abstract*: 243

The number of words in the *Introduction*: 542

The number of words in the *Discussion*: 2100

Abbreviations: AUC: area under the curve; CYP3A: cytochrome P450 3A; DDIs: drug-drug interactions; K_m: Michaelis-Menten constant; V_{max}: maximum rate of metabolism; K_I: concentration of inhibitor required for half maximal inactivation; k_{inact}: maximum inactivation rate constant; K_i: reversible inhibition equilibrium constant; k_{deg}: degradation rate constant of CYP3A; $f_{u,p}$: fraction unbound in plasma; $f_{u,mic}$: fraction unbound in liver microsomes; TDI: time dependent inhibitor; MBI: mechanism-based inhibitor; HLM: human liver microsome.

Abstract

Cryopreserved human hepatocytes suspended in human plasma (HHSHP) represent an integrated metabolic environment for predicting drug-drug interactions (DDIs). In this study, 13 CYP3A reversible and/or time dependent inhibitors (TDI) were incubated with HHSHP for 20 min over a range of concentrations after which midazolam 1'-hydroxylation was used to measure CYP3A activity. This single incubation time method yielded IC_{50} values for the 13 inhibitors. For each CYP3A inhibitor/victim drug pair, the IC_{50} value was combined with total average plasma concentration of the inhibitor in humans, fraction of the victim drug cleared by CYP3A and intestinal availability of the victim drug to predict the ratio of plasma area under the curve of the victim drug in the presence and absence of inhibitor. Of 52 clinical DDI studies utilizing these 13 inhibitors identified in the literature, 85% were predicted by this method within 2-fold of the observed change and all were predicted within 3-fold. Subsequent studies to determine mechanism (reversible and TDI) were performed by using a range of incubation periods and inhibitor concentrations. This system differentiated between reversible inhibitors, TDIs and the combination of both. When the reversible and inactivation parameters were incorporated into predictive models, 65% of 52 clinical DDIs were predicted within 2-fold of the observed changes and 88% were within 3-fold. Thus HHSHP produced accurate DDI predictions with a simple IC_{50} determined at a single incubation time regardless of the inhibition mechanism, further if needed, the mechanism(s) of inhibition can be identified.

DMD Fast Forward. Published on January 6, 2011 as DOI: 10.1124/dmd.110.036400
This article has not been copyedited and formatted. The final version may differ from this version.

Introduction

The inhibition of cytochrome P4503A (CYP3A) enzymes at the intestine and liver is responsible for many clinically important drug-drug interactions (DDIs) (Gomez et al., 1995; Gorski et al., 1998; Galetin et al., 2008). It is now a standard practice during drug development to predict the ability of candidate drugs to inhibit the cytochrome P450s, including CYP3As, using *in vitro* enzyme kinetic data generated from human liver microsomes (HLMs) (Bjornsson et al., 2003a; Bjornsson et al., 2003b). These *in vitro* CYP inhibition parameters have facilitated the assessment of risk and predicted the potential magnitude of DDI when combined with measures or predictions of human drug exposure but the approach is time consuming and has significant limitations. The state-of-the art prediction of an *in vivo* CYP-mediated, inhibitory DDI requires estimation of the reversible inhibition constant (K_i), the irreversible inhibition parameters (K_I and k_{inact}), the fraction unbound in plasma ($f_{u,p}$) and the fraction unbound in the microsomal system ($f_{u,mic}$) (Wang et al., 2004). Sophisticated models using static or dynamic drug concentration have been developed to integrate this data set and predict an *in vivo* DDI for a given drug dosing regimen (Obach et al., 2006; Einolf, 2007; Fahmi et al., 2009; Xu et al., 2009; Rowland Yeo et al., 2010). However, the resulting predictions often result in false positives, false negatives and fail to correctly categorize inhibitors as weak, moderate and strong *in vivo* inhibitors (Xu et al., 2009). Consequently, a consensus on the most appropriate predictive framework to be used during the development of a new drug candidate has not been reached.

Cryopreserved human hepatocytes suspended in well defined serum free media have been used to estimate TDI parameters for diltiazem, verapamil, erythromycin, clarithromycin, and troleandomycin, and combined with the Simcyp population-based ADME simulator to accurately predict CYP3A mediated DDIs (Xu et al., 2009). The value of this approach in predicting reversible inhibition was not assessed by these authors. Cryopreserved human hepatocytes suspended in human plasma (HHSHP) represent a convenient, integrated metabolic environment for estimating the extent and mechanism of human DDIs. Lu et al. (Lu et al., 2007; Lu et al.,

2008a; Lu et al., 2008b) have utilized the HHSHP system to quantitatively determine the inhibition of various P450s by ketoconazole and fluconazole. Using this information, CYP-mediated changes in the area under the curve (AUC) of several victim drugs were predicted accurately for DDIs involving these two prototypical competitive inhibitors, but the applicability to mechanism based inhibitors (MBI) was not addressed. Compared to in vitro systems using HLM, human hepatocytes suspended in human plasma inherently account for several parameters: 1) the plasma protein and microsomal binding of drug, 2) compound availability to the enzyme in its native environment within the cell and 3) metabolism of the compound by both CYP and non-CYP pathways including the potential for the formation of inhibitory metabolites.

The primary objective of the current study using HHSHP is to quantify the ability of a simple, single incubation time method to assess the CYP3A inhibition by a test compound in order to predict clinical DDIs without the knowledge of inhibition mechanism. A secondary aim is to identify the inhibition mechanism and compare the clinical DDI prediction based on the appropriate mechanistic models to those from the single incubation time method.

Materials and Methods

Materials. Cryopreserved human hepatocytes and InVitro GRO^{TM} HT Medium were obtained from Celsis In Vitro Technologies, Inc. (Baltimore, MD). Midazolam, 1'-hydroxymidazolam (1' OH midazolam) and [$^{13}C_5$]-1'-hydroxymidazolam were obtained from BD Gentest (Woburn, MA). Conivaptan was obtained internally. Clarithromycin, diltiazem, erythromycin, fluconazole, itraconazole, ketoconazole, nefazodone, and troleandomycin were obtained from Sigma (St. Louis, MO). Aprepitant, ritonavir, saquinavir, and voriconazole were obtained from Toronto Research Chemicals (North York, ON, Canada). Human plasma (Na-heparin) was obtained from Lampire Biological Laboratories, Inc. (Pipersville, PA). Hepatocyte Maintenance Medium (HMM) was obtained from Lonza, Inc. (Walkersville, MD).

Hepatocyte studies. Hepatocytes (pool of five individuals) were thawed in InVitro GRO^{TM} HT Medium (25 ml per 5 million hepatocytes) and centrifuged at 50*g* at room temperature for 5 min. The cell pellet was reconstituted in HMM, and cell viability was found to be at least 80% using a Vi-Cell XR cell viability analyzer (Beckman Coulter Inc., Brea, CA). After the cell viability was determined, hepatocytes were centrifuged at 50*g* at room temperature for 5 min and resuspended in human plasma ($2x10^6$ cells/ml). The cell suspension was incubated at 37 °C with 5% CO_2 until the addition of putative enzyme inhibitors.

Inhibition studies. The final inhibitor concentrations in human plasma were 0.13-100 µM for aprepitant, fluconazole, voriconazole, clarithromycin, conivaptan, diltiazem, erythromycin, itraconazole, nefazodone and troleandomycin, 0.03-20 µM for ketoconazole and ritonavir, and 0.07 to 50 µM for saquinavir. The final organic vehicle concentration was 0.5% methanol. The incubations were performed in triplicate. Stock hepatocyte suspension (25 µl) was added to 50 µl of inhibitor-containing plasma such that the final concentration of hepatocytes was 0.5×10^6 cells/ml in human plasma and incubated for 20 min. (37 °C, 5% CO_2) before the addition of midazolam. To assess the effect of incubation time, cells were incubated with inhibitors for 0, 10, and 20 min. prior to the addition of midazolam. Midazolam (25 µl in human plasma; final

DMD Fast Forward. Published on January 6, 2011 as DOI: 10.1124/dmd.110.036400
This article has not been copyedited and formatted. The final version may differ from this version.

concentration = 30 μM) was added to the cell suspension, and a further 35 min of incubation was used to quantify the remaining CYP3A activity. The reactions were terminated by adding 200 μl of acetonitrile/methanol (3:1 v/v) containing 150 nM [$^{13}C_5$] -1'-OH midazolam as an internal standard. Samples were centrifuged at 4000 rpm for 20 min and an aliquot of the supernatant was analyzed by LC-MS/MS. Preliminary experiments demonstrated that these incubation conditions resulted in linear formation of 1'-hydroxymidazolam with respect to the incubation time and the hepatocyte concentration. The formation of 1'-hydroxymidazolam was linear for 80 minutes.

Liquid chromatography/tandem mass spectrometry methods. Quantification of 1'-OH midazolam was achieved using HPLC (Shimadzu LC10) interfaced to a triple quadrapole mass spectrometer (Sciex API 4000, Applied Biosystems, Foster City, CA). Chromatographic separation was achieved using a reverse phase column (Synergi Hydro-RP 4 μm column, 100 × 2 mm, Phenomenex, Torrance, CA) with a gradient consisting of 5% methanol in 5 mM ammonium acetate (mobile phase A) and 95% methanol in 5 mM ammonium acetate (mobile phase B) at a flow rate of 0.4 mL/min with a 25 μl injection volume. Specifically, 70% of mobile phase B was increased linearly to 80% from 0 to 2 min, and increased to 100% in the next 0.05 min. Mobile phase B was held at 100% from 2.05 to 2.30 min, and the column was re-equilibrated to 70% B. The electrospray ionization probe was run in the positive ion mode with probe temperature of 600 °C. The *m/z* transition of 1'-OH midazolam and [$^{13}C_5$]-1'-OH midazolam were 342 →324 and 347 →329, respectively. The lower and upper limits of quantification were 0.5 and 234 pmol 1'-OH midazolam, respectively, per 100 μL well incubation. The interday accuracy ranged from -4.97% to 10.26%, and the intraday accuracy ranged from -6.13% to 11.09%. The interday precision ranged from 2.47% to 8.15%, and the intraday precision ranged from 1.70% to 13.15%.

Data analysis.

Inhibition data. The relationship between CYP3A activity at a given time and inhibitor concentration relative to baseline CYP3A activity was used to determine an IC_{50}. All data were

DMD Fast Forward. Published on January 6, 2011 as DOI: 10.1124/dmd.110.036400
This article has not been copyedited and formatted. The final version may differ from this version.

analyzed using the average of triplicate determinations. IC_{50} values were calculated by the model (Eq. 1) by weighted nonlinear regression (WinNonlin 5.0, Pharsight Corp, Mountain View, CA).

$$Y = \frac{a}{\gamma \times (X/IC_{50}) + 1} \quad \text{(Eq. 1)}$$

Where X is the nominal concentration of an inhibitor; Y represents the percentage of baseline CYP3A activity remaining; a is the estimated response at zero concentration of inhibitor; γ is the slope factor, describes the steepness of the curve.

Three inhibition models incorporating irreversible (Model B), reversible (Model C), or both (Model A), were employed to estimate the inactivation parameters (K_I and k_{inact}) and/or reversible inhibition constant (K_i) for each inhibitor when three IC_{50} curves obtained from different incubation times were simultaneously fitted using weighted nonlinear regression. The most appropriate model was chosen using the following goodness of fit criteria: visual inspection, randomness of the residuals, and the standard error of the parameter estimates.

Model A:
$$\frac{V_{35+t,[I]}}{V_{35+t,[0]}} = \frac{[S] \times V_{max,\,35+t} \times e^{-(\frac{k_{inact} \times [I]}{K_I + [I]}) \times (35+t)}}{\{K_{m,\,MDZ} \times (1 + [I]/K_i) + [S]\} \times V_{35+t,[0]}} \quad \text{(Eq. 2)}$$

Model B:
$$\frac{V_{35+t,[I]}}{V_{35+t,[0]}} = \frac{[S] \times V_{max,\,35+t} \times e^{-(\frac{k_{inact} \times [I]}{K_I + [I]}) \times (35+t)}}{\{K_{m,\,MDZ} + [S]\} \times V_{35+t,[0]}} \quad \text{(Eq. 3)}$$

Model C:
$$\frac{V_{35+t,[I]}}{V_{35+t,[0]}} = \frac{[S] \times V_{max,\,35+t}}{\{K_{m,\,MDZ} \times (1 + [I]/K_i) + [S]\} \times V_{35+t,[0]}} \quad \text{(Eq. 4)}$$

In Eq. 2-4, t is the time during which the inhibitors are in contact with human hepatocytes prior to the addition of midazolam (0, 10 or 20 min). $V_{35+t,\,[I]}$ represents the formation rate of 1'-OH midazolam at a given concentration of the inhibitor and total time (total time = 35 min with midazolam plus t min without midazolam), and $V_{35+t,\,[0]}$ is the formation rate of 1'-OH midazolam for the corresponding vehicle control (no inhibitor) at the same incubation time. The ratio of $V_{35+t,\,[I]}$ and $V_{35+t,\,[0]}$ normalizes the baseline for the enzyme activity for the specific incubation time. K_m

DMD Fast Forward. Published on January 6, 2011 as DOI: 10.1124/dmd.110.036400
This article has not been copyedited and formatted. The final version may differ from this version.

is the Michaelis-Menten constant for 1'-OH midazolam formation in HHSHP (45 μM, based on total and not unbound midazolam concentration, data not shown), and [S] is midazolam concentration (30 μM). $V_{max,\ 35\ +t}$ represents maximum rate of 1'-OH midazolam formation at some total time. The rate of 1'-OH midazolam formation varied with incubation time and consequently the ratio of $V_{max,\ 35\ +t}$ and $V_{35+t,\ [0]}$ was estimated by Models A-C (Eq. 2-4). [I] is the nominal inhibitor concentration, assuming no inhibitor depletion during the incubation. K_I is the inhibitor concentration required for the half maximal inactivation, k_{inact} is the maximum inactivation rate constant, and K_i is the reversible inhibition equilibrium constant.

All raw data were fitted to Model A. If the parameters K_i, k_{inact} and K_I with less CV% were estimated by Model A from the simultaneous fitting three sets of data corresponding to the ratio of 1'-OH midazolam formation rate versus inhibitor concentrations using weighted nonlinear regression, it suggested that the compound is a reversible and time dependent inhibitor. For compounds which Model A was able to estimate the inactivation parameters (K_I and k_{inact}) but not the reversible inhibition constant K_i, the raw data were fitted to Model B which only estimates the inactivation parameters (K_I and k_{inact}). For compounds which Model A was able to estimate the reversible inhibition constant K_i but not the inactivation parameters (K_I and k_{inact}), the raw data were fitted to Model C which only estimates the reversible inhibition constant K_i.

Predictions of drug-drug interactions.

The single incubation time method A generic model (Eq. 5) of enzyme inhibition was used to predict a potential increase in exposure to a drug as a result of the inhibition of hepatic and intestinal CYP3A (Ito et al., 1998; Wang et al., 2004; Obach et al., 2006). All assays were performed at a substrate concentration close to the K_m of midazolam (data not shown). The inhibition mechanism may be unknown for some inhibitors nevertheless the assumption that $K_{i,\ app} = IC_{50}/2$ was applied (Obach et al., 2007). For competitive inhibitors, the $K_{i,\ app}$ would be equivalent to the inhibition constant K_i. In the case of TDIs that display mechanism based inhibition, $K_{i,\ app}$ would be equivalent to $K_I \times k_{deg} / k_{inact}$ when $[I] << K_I$ (Wang et al., 2004).

DMD Fast Forward. Published on January 6, 2011 as DOI: 10.1124/dmd.110.036400
This article has not been copyedited and formatted. The final version may differ from this version.

$$\frac{AUC_{p.o.,i}}{AUC_{p.o.}} = \frac{CL_{u,int}}{CL_{u,int,i}} = \frac{1}{[f_{m,CYP3A}/(1+[I]/K_{i,app})]+(1-f_{m,CYP})} \times \frac{1}{[(1-F_g)/(1+[I]_g/K_{i,app} \times f_{u,p})]+F_g} \quad \text{(Eq. 5)}$$

Where $AUC_{p.o.,i}/AUC_{p.o}$ is the predicted ratio of *in vivo* exposure of a CYP3A-cleared drug with oral coadministration of the inhibitor versus that in control state, $f_{m,CYP3A}$ is the fraction of total clearance of the affected drug to which CYP3A contributes, F_g is the fraction of the dose of the affected drug that passes through the intestine unchanged after p.o. administration in the control state.

The fraction of object drug metabolized by CYP3A ($f_{m,CYP3A}$) was assumed to be the same as that observed previously for midazolam, sildenafil, fentanyl, triazolam, zolpidem, alprazolam and trazadone (0.93, 0.79, 0.5, 0.8, 0.6, 0.8, and 0.35, respectively) (Obach et al., 2006). The fraction of drug metabolized by CYP3A in the intestine was assumed to be 1, and the Fg values for midazolam, sildenafil, triazolam, alprazolam and trazadone were assumed to be 0.57, 0.38, 0.44, 0.88 and 0.75 respectively, as described previously (Ernest et al., 2005; Obach et al., 2006). [I] is collected from three main sources (details in the Supplemental Table 1). The average systemic plasma concentration of the inhibitor (plasma concentration area under curve from 0 to the dosing interval ($AUC_{0-\tau}$) divided by the dosing interval) observed or calculated in the primary literature was preferred. In some cases this was not available and then the plasma inhibitor concentration at a certain time point (eg. when the victim drug was administered) reported in the primary literature was employed. If the inhibitor concentration was not reported in the primary literature, values were obtained from secondary literature sources (Einolf, 2007; Fahmi et al., 2008; Fahmi et al., 2009). These values were previously derived from other literature in which similar dosing regimens were employed for individual inhibitors. The IC_{50} values are based on total inhibitor concentration in plasma and consequently there is no need to use unbound

DMD Fast Forward. Published on January 6, 2011 as DOI: 10.1124/dmd.110.036400
This article has not been copyedited and formatted. The final version may differ from this version.

plasma concentrations in the predictions. For the prediction of intestinal inhibition, $K_{i,app}$ values were converted to unbound values ($K_{i,app} \times f_u$) consistent with the assumption of no significant protein binding in the gut lumen. The fraction unbound in human plasma for each compound was taken from Goodman & Gilman (Hardman et al., 2001).

The concentration of the inhibitor in the enterocyte during absorption ($[I]_g$) was estimated based on the assumption that 1) no significant protein binding in the gut lumen and 2) inhibitors not subject to any first pass metabolism (Rostami-Hodjegan A, 2004; Galetin et al., 2008):

$$[\mathrm{I}]_g = \frac{\mathrm{D} \times k_a \times F_a}{Q_{ent} \times MW} \qquad \text{(Eq. 6)}$$

In which D is the dose of the inhibitor (mg), k_a is the oral absorption rate constant of the inhibitor, F_a is the fraction of the inhibitor absorbed into the gut wall from the intestinal lumen following oral administration, Q_{ent} represents the blood flow to the enterocyte, and MW is the molecular weight. For k_a and Q_{ent} values of 0.03 min^{-1} and 248 ml/min were used, respectively (Obach et al., 2006). An F_a value of 1 was used for all drugs (Einolf, 2007).

In the current investigation, there were 12 clinical studies in which victim drugs were given intravenously. Among these 12 studies, midazolam was the victim drug in eleven clinical studies and the inhibitors were ketoconazole, aprepitant, conivaptan, voriconazole, troleandomycin, erythromycin, clarithromycin, diltiazem and saquinavir. In the other clinical study, fentanyl was the victim drug and ritonavir was the inhibitor. For these 12 studies, the AUC ratio was predicted using Eq. 7, in which the hepatic extraction ratio (EH) of the victim drug is accounted for in the DDI prediction (Kirby and Unadkat, 2010). Midazolam was assignedan EH of 0.4 (mean value calculated from the eleven clinical studies) and fenatanyl was assigned a value of 0.7 (Olkkola et al., 1999).

$$\frac{AUC_{IV,i}}{AUC_{IV}} = EH \times [(\frac{1}{EH} - 1) \times \frac{1}{\left((1 - fm_{CYP3A}) + \frac{fm_{CYP3A}}{1 + \left(\frac{[I]}{K_i} \right)} \right)} + 1] \qquad \text{(Eq. 7)}$$

DMD Fast Forward. Published on January 6, 2011 as DOI: 10.1124/dmd.110.036400
This article has not been copyedited and formatted. The final version may differ from this version.

The mechanistic method According to the inhibition mechanism, the magnitude of DDIs involving each inhibitor was predicted using the appropriate models.

For drugs identified as reversible inhibitors, AUC ratios were calculated by Eq. 5, where $K_{i,app}$ was equal to the K_i estimated by Model C.

For drugs identified as TDIs with Model B, AUC ratios were calculated using the following equation (Mayhew et al., 2000; Wang et al., 2004).

$$\frac{AUCp.o.,i}{AUCp.o} = \frac{1}{\left(1-fm_{CYP3A}\right)+\dfrac{fm_{CYP3A}}{1+\left(\dfrac{k_{inact}\times[I]}{(K_I+[I])\times k_{\deg,CYP3A,h}}\right)}} \times \frac{1}{\left(F_g+\left(1-F_g\right)\times\dfrac{1}{1+\dfrac{k_{inact}\times[I]_g}{(K_I\times f_{u,p}+[I]_g)\times k_{\deg,CYP3A,g}}}\right)} \quad \text{(Eq. 8)}$$

where k_{deg} is the first-order rate constant of *in vivo* degradation of the affected enzyme. The values of k_{deg} used for intestinal ($k_{deg,CYP3A,g}$) and hepatic CYP3A ($k_{deg,CYP3A,h}$) were 0.000481 ($t_{1/2}$ = 24 h) and 0.000321 min $^{-1}$ ($t_{1/2}$ = 36 h), respectively (Wang et al., 2004; Obach et al., 2007; Quinney et al., 2010; Wang, 2010). For the 12 clinical studies involving IV administration of the victim drug, the AUC ratio was predicted using Eq. 9 (Kirby and Unadkat, 2010).

$$\frac{AUC_{IV,i}}{AUC_{IV}} = EH\times\left[\left(\frac{1}{EH}-1\right)\times\frac{1}{\left(1-fm_{CYP3A}\right)+\dfrac{fm_{CYP3A}}{1+\left(\dfrac{k_{inact}\times[I]}{(K_I+[I])\times k_{\deg,CYP3A,h}}\right)}}+1\right] \quad \text{(Eq. 9)}$$

For drugs identified as reversible and time dependent inhibitors with Model A, the AUC ratio was calculated using Eq. 9 (Fahmi et al., 2008). For the ritonavir and IV fentanyl DDI, the AUC ratio was predicted using Eq. 11 (Kirby and Unadkat, 2010).

DMD Fast Forward. Published on January 6, 2011 as DOI: 10.1124/dmd.110.036400
This article has not been copyedited and formatted. The final version may differ from this version.

$$\frac{AUCp.o.,i}{AUCp.o} = \frac{1}{\left(1 - fm_{CYP3A}\right) + fm_{CYP3A} \times \left(\frac{1}{1 + \left(\frac{k_{inact} \times [I]}{(K_I + [I]) \times k_{deg,CYP3A,h}}\right)} \times \frac{1}{1 + [I]/Ki}\right)} \times \frac{1}{F_g + \left(1 - F_g\right) \times \left(\frac{1}{1 + \frac{k_{inact} \times [I]_g}{(K_I \times f_{u,p} + [I]_g) \times k_{deg,CYP3A,g}}} \times \frac{1}{1 + [I]_g/(Ki \times f_{u,p})}\right)}$$

(Eq. 10)

$$\frac{AUC_{IV,i}}{AUC_{IV}} = EH \times \left[\left(\frac{1}{EH} - 1\right) \times \frac{1}{\left(1 - fm_{CYP3A}\right) + \frac{fm_{CYP3A}}{\left(1 + \left(\frac{[I]}{K_i}\right)\right) \times \left(1 + \left(\frac{k_{inact} \times [I]}{(K_I + [I]) \times k_{deg,CYP3A,h}}\right)\right)}} + 1\right] \quad \text{(Eq. 11)}$$

Data source. Data from fifty two clinical DDI studies were collected from the literature after having been identified by the University of Washington Metabolism and Transport Drug Interaction Database (http://www.druginterationinfo.org/). Forty six clinical DDI studies involved the inhibition of midazolam metabolism, 5 studies involved the inhibition of alprazolam, fentanyl, sildenafil, trazadone and triazolam metabolism by ritonavir; 1 study involved the inhibition of sildenafil by saquinavir. The database was accessed on 01/29/2009, and the data are reported in Table 3.

Data analysis. Among 52 clinical DDIs, there are 22 strong interactions (AUC ratio > 5), 26 moderate interactions (2 ≤ AUC ratio ≤ 5) and 4 weak interactions (1 ≤AUC ratio < 2). Two methods were employed to quantify the accuracy of predicted DDIs. One is to compare the fold error of predicted and observed values of AUC ratio (2-fold cut-off). Another method is called "categorical prediction" based on the definition of strong interactions, moderate interactions and weak interactions.

DMD Fast Forward. Published on January 6, 2011 as DOI: 10.1124/dmd.110.036400
This article has not been copyedited and formatted. The final version may differ from this version.

Results

Enzyme inhibition parameter estimation

The thirteen known CYP3A inhibitors represented reversible inhibitors (ketoconazole as strong reversible inhibitor and fluconazole as a moderate inhibitor) and TDIs (TAO as a strong TDI, diltiazem as a moderate TDI, and erythromycin as a weak TDI) that displayed a wide range of plasma protein binding (itraconazole and ketoconazole high protein binding, voriconazole and clarithromycin moderate protein binding, and fluconazole low protein binding). These inhibitors were incubated with human hepatocytes suspended in human plasma for 20 min over a range of concentrations in the absence of midazolam and a further 35 min in the presence of midazolam (30 μM). The IC_{50} value for each inhibitor was estimated using Eq. 1 and the values are shown in Table 1. For ketoconazole and fluconazole, the IC_{50} values obtained here were similiar to those observed by Lu et al. using a comparable procedure (Lu et al., 2007; Lu et al., 2008a; Lu et al., 2008b). Based on the assumption that the nominal concentration of inhibitor is close to the extracellular concentration, these IC_{50} values represent the total (bound and unbound) concentration of the inhibitors that inhibit 50% of CYP3A activity and consequently there was no correction of fraction unbound in plasma for the IC_{50} values. As shown in Table 1, ritonavir was the most potent inhibitor with the lowest IC_{50} value, while aprepitant had the highest IC_{50} value among the 13 drugs studied. In additional studies, incubation times of 0, 10 and 20 min (with inhibitors alone) were used to generate IC_{50} values (Table 1). The IC_{50} value at the 20 min in the two independent studies showed very good agreement (Table 1).

To define the inhibition mechanism for each inhibitor, models of reversible inhibition (Model C), irreversible inhibition (Model B), and combined reversible and irreversible inhibition (Models A) were employed (Eq. 3-5). Examples of the results of the best fit of four representative drugs (ketoconazole, erythromycin, itraconazole and ritonavir) are shown in Fig. 1a-d, and the *in vitro* inhibition constants for each inhibitor obtained from the best model fit analyses are listed in

Table 2. The process of defining the inhibition mechanism took place in the following three steps. First, all raw data were fitted to the combined reversible plus irreversible model (Model A). The fit of Model A indicated that ketoconazole is a reversible inhibitor but not a TDI because Model A was able to estimate the reversible inhibition constant K_i but not the inactivation parameters (K_I and k_{inact}). This observation was also the case with fluconazole, aprepitant and voriconazole, which is not unexpected because these compounds are all known reversible inhibitors (Ito et al., 1998). A second group of compounds (erythromycin, nefazodone, troleandomycin, clarithromycin, diltiazem, itraconazole and saquinavir) were identified as TDI only, because Model A was able to estimate the inactivation parameters (K_I and k_{inact}) for each with reasonable precision but not the reversible inhibition constant K_i. Ritonavir represents a potential third group of compounds as it was suggested to be a reversible and time-dependent inhibitor because both the reversible inhibition constant K_i and the inactivation parameters (K_I and k_{inact}) were well estimated (Fig. 1d and Table 2).

In the second step of assigning a mechanism, inhibitors which were initially assigned as TDIs only were further analyzed using the model for irreversible inhibition (Model B), which only estimates the inactivation parameters (K_I and k_{inact}). Better fitting of the data and more precise (less CV%) estimates of inactivation parameters of these inhibitors (TDI only) were obtained utilizing Model B (Fig. 1b-c and Table 2). For example, the fit of erythromycin to model A resulted in the mean estimate and the standard error of the estimates of k_{inact}, K_I and K_i as 0.08 ± 0.07 min^{-1} (87.50 % CV), 35.09 ± 31.92 μM (90.97 % CV) and 497.65 ± 8311.13 μM (1670.09 % CV), where as the results were significantly better when the data were fit to model B yielding the values of k_{inact} and K_I as 0.08 ± 0.005 min^{-1} (6.25 % CV) and 25.15 ± 4.90 μM (19.48 % CV), respectively. In the third step, inhibitors which were identified as purely reversible inhibitors in the first step were analyzed using Model C, which only estimates the reversible inhibition constant K_i. Better fitting of the data and more precise (less CV%) estimates

of K_i for these inhibitors were obtained utilizing Model C (Fig. 1a and Table 2). For example, the fit of ketoconazole to model A resulted in the mean estimate and the standard error of the estimates of k_{inact}, K_I and K_i as 0.000003 ± 0.2 min^{-1} (7686821 % CV), 32.67 ± 8543863 μM (10845820 % CV) and 0.61 ± 0.18 μM (29.51 % CV), where as the results were significantly better when the data were fit to model C yielding the value of K_i as 0.59 ± 0.09 μM (15.25 % CV). In addition, Model C also fitted the ritonavir data well, which was not surprising as the compound was reported as a very potent reversible as well as a TDI in HLM (Ernest et al., 2005). Thus, the inhibition constants of ritonavir estimated from both models have been included in Table 2.

Prediction of DDIs

The *in vitro* inhibition constants for the thirteen CYP3A inhibitors studied were used to predict 52 clinical DDIs (Table 3) using the single incubation time method and mechanistic method. In these studies, for 12 of the 13 inhibitors the victim drug was midazolam; for ritonavir the victim drugs were sildenafil, fentanyl (intravenous), triazolam, alprazolam and trazodone; for saquinavir one of the victim drugs was sildenafil.

The single incubation time method: IC_{50} values from a 20 min incubation with inhibitor alone

IC_{50} values from a 20 min incubation time with inhibitor and a further 35 min of incubation with midazolam were converted to $K_{i,app}$ ($K_{i,app}$=IC_{50} / 2) and used in Eq. 5 to predict the extent of DDI *in vivo*. The total average systemic plasma concentration of each inhibitor was employed as [I] because *in vitro* parameters were estimated relative to total plasma concentration there was no need for correction for the fraction unbound in plasma for [I] (Table 3); $[I]_g$ was calculated using Eq.6. The predicted and observed AUC ratios are listed in Table 3, and a plot of predicted DDIs versus observed values from clinical studies is shown in Fig 2. The single incubation time method correctly classified DDIs in 12 out of 20 strong interactions (60% accuracy), 15 out of 28 moderate interactions (54% accuracy) and 4 out of 4 weak

interactions (100% accuracy) (Fig. 2). Using the criteria of within 2-fold of the observed value for an accurately predicted DDI, this approach correctly predicted 44 out of 52 clinical DDIs (85% accuracy) (Fig. 2). The predictions for the remaining outliners (8 out of 52) were within-3 fold of the observed values and included 2 cases for fluconazole, 2 case for voriconazole, 2 cases for saquinavir, and 2 cases for clarithromycin. There were no false positive or false negative predictions.

The mechanistic method: utilizing in vitro parameters estimated by Models A-C

As described in Materials and Methods, each DDI was also predicted according to the inhibition mechanism of the compound. The magnitude of DDIs for the four reversible inhibitors (ketoconazole, aprepitant, fluconazole and voriconazole identified by Model C) was predicted by Eqs. 5 and 7. DDIs with the 8 TDI inhibitors (troleandomycin, saquinavir, clarithromycin, conivaptan, diltiazem, erythromycin, itraconazole and nefazodone identified by Model B) were predicted by Eqs. 8 and 9. DDIs with ritonavir, which was identified as a reversible and time dependent inhibitor by Model A, were predicted by Eqs. 10 and 11. Total average systemic plasma concentration of each inhibitor was used as [I] because *in vitro* parameters were estimated relative to total plasma concentration (Table 3); $[I]_g$ was calculated using Eq.6. Predicted AUC ratios are listed in Table 3, and plots of predicted DDIs versus observed values from clinical studies are shown in Fig 3. This approach correctly classified DDIs in 18 out of 20 strong interactions (90% accuracy), 4 out of 28 moderate interactions (14% accuracy) and 3 out of 4 weak interactions (75% accuracy), respectively (Fig. 3). This approach predicted 34 out of 52 clinical DDIs (65% accuracy) within 2-fold of the observed AUC changes and 46 out of 52 clinical DDIs (88% accuracy) within 3-fold (Fig. 3). Predictions that were more than 3-fold different from observed values involved 1 case for saquinavir, 1 cases for erythromycin, 1 case for clarithromycin, 1 case for diltiazem and 2 cases for conivaptan. There were no false positive or false negative predictions.

Predictive performance of the single incubation time method for each of the three inhibition mechanisms

Eight inhibitors were identified as TDIs by Model B, and the single incubation time method correctly classified the DDI caused by these 8 TDIs in 4 out of 10 strong interactions (40% accuracy); 9 out of 19 moderate interactions (47% accuracy) and 1 out of 1 weak interactions (100% accuracy). For 4 reversible inhibitors, the single incubation time method correctly classified the DDIs in 6 out of 8 strong interactions (75% accuracy); 4 out of 6 moderate interactions (67% accuracy) and 3 out of 3 weak interactions (100% accuracy). For ritonavir, the single incubation time method correctly classified DDIs in four interactions (75% accuracy). When the 2-fold cut-off criteria was used to evaluate the performance of the single incubation time method, 25 out of 30 clinical DDIs were predicted correctly for TDIs (83% accuracy), 14 out of 17 clinical DDIs were predicted correctly for reversible inhibitors (82% accuracy), and 5 out of 5 clinical DDIs were predicted correctly for reversible and time dependent inhibitor ritonavir (100% accuracy). This retrospective analysis suggested that the single incubation time method was a strong predictor of DDIs due to TDIs as well as reversible inhibitors when the 2-fold criterion was used.

Discussion

Hepatocytes obtained in well defined serum free media have previously been demonstrated to be a useful system for the estimation of CYP3A inhibition parameters (Zhao et al., 2005; McGinnity et al., 2006; Brown et al., 2007; Xu et al., 2009). Zhao et al. (2005) evaluated time dependent inactivation of CYP3A in cryopreserved human hepatocytes for six drugs (amprenavir, diclofenac, diltiazem, erythromycin, raloxifene and TAO), and the IC_{50} values for hepatocytes were 2- to 60-fold higher than those for HLM after correcting for factors such as nonspecific binding and inhibitor consumption in hepatocytes. McGinnity et al. (2006) incubated three CYP3A inhibitors (erythromycin, TAO and fluoxetine) with cultured primary human hepatocytes for 48 hours, and the parameters associated with irreversible inhibition were in good agreement with those generated with HLM although lower values of k_{inact} were observed in both Hepatocytes and HLM systems compared to the recombinant CYP3A. Brown et al. (2007) investigated six drugs (miconazole, ketoconazole, fluconazole, quinine, fluoxetine and fluvoxamine) in both rat micosomes and freshly isolated rat hepatocytes, and indicated that these systems gave similar estimates of inhibitory potency after correction for the nonspecific binding in each system for these CYP3A inhibitors. However, although all three studies noted above (Zhao et al., 2005; McGinnity et al., 2006; Brown et al., 2007) compared the *in vitro* inhibition parameters generated from microsomes to those from hepatocytes, the question of whether the parameters generated from hepatocytes resulted in an improved ability to predict human DDIs was not addressed. Xu et al. (2009) noted that the values of k_{inact} in HLM were higher and the values of unbound K_I in HLM were lower than those estimated in cryopreserved human hepatocytes. The *in vitro* inactivation parameters from cryopreserved human hepatocytes resulted in good overall prediction of *in vivo* DDI extent but there was a systematic over prediction with HLM data (Xu et al., 2009), and both hepatocyte and HLM prediction resulted in several false negative predictions. Lu et al. expanded the utility of cryopreserved human hepatocytes by using a suspension in human plasma and demonstrated a good agreement between predicted and

observed clinical DDIs involving two known CYP3A inhibitors, ketoconazole and fluconazole (Lu et al., 2007; Lu et al., 2008a; Lu et al., 2008b). In the present report, the utility of cryopreserved human hepatocytes suspended in human plasma to predict *in vivo* DDIs was further explored using 13 reversible and TDIs of CYP3A and midazolam as the probe substrate.

The approach to predict CYP3A DDI prediction utilized in the current report did not focus on an initial characterization of the mechanism of inhibition but rather employed a single IC_{50} measurement in hepatocytes suspended in human plasma; an analogous approach has been described in the HLM system (Obach et al., 2007; Grime et al., 2009; Burt et al., 2010). This single incubation time method captures both reversible and TDI by using appropriate experimental conditions. In these studies, $0.5x10^6$ cryopreserved hepatocytes per ml were used because this is similar to 0.17 mg/ml HLM protein, a concentration commonly used in studies in HLMs (based on the scaling factors of 120 x 10^6 hepatocytes cells/g liver and 40 mg HLM/g liver). The inhibitor-alone incubation time with hepatocytes was 20 min and this would be expected to result in almost complete CYP3A inactivation given a typical HLM k_{inact} value of approximately 0.1 min^{-1}. However, it should be noted that the values of k_{inact} of clarithromycin and saquinavir were 0.064 and 0.033, respectively ($t_{1/2}$ respectively of 11.55 min and 20.02 min), and these relatively low values likely contributed to the DDI under-prediction for these two compounds (Table 3). The concentration of midazolam, employed to determine residual CYP3A activity (30 μM), was close to the K_m value of 45 μM in HHSHP (preliminary experiments, and the estimate is based on total and not unbound midazolam concentration) to capture reversible inhibition in the IC_{50} measurement. The formation of 1'-hydroxymidazolam over a 35 min incubation time was used the quantify CYP3A activity. Under these conditions, metabolite formation was linear over time and yielded sufficient analytical response to characterize extensive CYP3A inhibition.

The results presented demonstrate that an IC_{50} value generated from a single incubation time was able to adequately predict the magnitude of an *in vivo* DDI (Table 3, Fig. 2). This IC_{50}

value is combined with the total average systemic plasma concentration of the inhibitor in a predictive model that incorporates the fraction of the victim drug cleared by CYP3A, and intestinal availability of the victim drug (Eq. 5). This differs from previous approaches wherein the mechanism(s) of inhibition needs to be identified prior to the parameter estimation *in vitro* and DDI prediction *in vivo*. This single incubation time method was able to predict 85 % of 52 clinical CYP3A DDI studies within 2-fold of the observed change in AUC regardless of the inhibition mechanism (Fig. 2). The high rate of successful prediction of DDI suggests that this relatively simple, mechanism independent approach will be of great use to determine the potential for CYP3A mediated DDIs for new candidates and previously uncharacterized molecules. This single incubation time approach to predicting DDIs may be particularly useful for molecules with a potential for exhibiting TDI in the early discovery stage when the standard time-consuming process of estimating the inactivation parameters (K_I and k_{inact}) in HLM may not be feasible. Although the single time point method may not provide the inhibition mechanism, it was able to accurately predict the DDIs related to 8 TDIs. Among these 8 TDIs, itraconazole is believed to exhibit TDI due to the inhibitory metabolite formation (Isoherranen et al., 2004; Kunze et al., 2006; Quinney et al., 2008a; Templeton et al., 2008) whereas the remaining seven TDIs were known to display MBI. The potential of predicting the interaction due to the inhibitory metabolite formation without synthesizing and testing the metabolite is an important feature of this model particularly useful in the discovery phase of the development of a new chemical entity, since identification of the exact structure of the metabolite often may not be available in early discovery.

It is well known that the expression of CYP3A enzymes in enterocytes results in significant presystemic intestinal metabolism of drugs and possible gut wall DDIs after oral administration (Schwenk, 1988; Kaminsky and Fasco, 1991; Paine and Oberlies, 2007). Clinical studies included in the dataset used in this investigation showed that ketoconazole, voriconazole,

troleandomycin, erythromycin, clarithromycin, diltiazem and conivaptan treatments led to a higher AUC increase for oral midazolam than for intravenous midazolam. These observations are consistent with significant inhibition of gut wall CYP3A given that midazolam is a drug with a moderate hepatic extraction ratio. The single incubation time method showed accurate prediction for both intravenous and oral midazolam AUC changes with erythromycin, clarithromycin, diltiazem, TAO and conivaptan. For example, clarithromycin administration (500 mg bid for 7 days) led to an increase in the AUC of midazolam by 3.20-fold following intravenous dosing and 8.00-fold following oral dosing (Quinney et al., 2008b). The corresponding predictions using the single incubation time method were 2.47-fold and 6.18-fold increases in midazolam AUC, respectively. In some cases, the oral midazolam DDI (e.g. ketoconazole) has not been well predicted. The reason for such an outcome is that the value of 0.57 which has been used as F_g for midazolam in this investigation (Ernest et al., 2005; Obach et al., 2006) is higher than the true value observed in some of clinical DDI studies. For instance, Tsunoda et. al. (1999), estimated the F_g value for midazolam to be 0.40 (assuming Fa=1). In order to illustrate the impact of F_g value to the DDI prediction outcome, another set of DDI predictions based on $F_{g,\ midazolam}$ = 0.40 was constructed (Fig. 4a). The clinical studies with victim drugs other than midazolam were excluded from this figure. For the eleven clinical studies in which midazolam was dosed intravenously, the difference in $F_{g,\ midazolam}$ would not influence the outcome of these DDI predictions. When $F_{g,\ midazolam}$ = 0.40 was used, it was found that 38 out of 46 clinical DDIs were predicted within 2-fold of the observed value (83% accuracy), 44 out of 46 within 3-fold of the observed value (95% accuracy), and only 2 out of 46 have been slightly overpredicted beyond the 3-fold range. For the ketoconazole-midazolam interaction from Tsunoda et. al. (1999), the prediction was improved from 8.47 to 12.05 and is closer to the observed value of 16-fold AUC change due to a better representation of the intestinal interaction when $F_{g,\ midazolam}$ = 0.40. This example reinforces the concept that it is not only the *in vitro* inhibition parameters that influence the quality of the final

DMD Fast Forward. Published on January 6, 2011 as DOI: 10.1124/dmd.110.036400
This article has not been copyedited and formatted. The final version may differ from this version.

DDI prediction, but also whether the pharmacokinetic parameters utilized in the model (F_g and f_m for the victim drug) represent the population in a specific clinical DDI study.

Although there is no need to correct the systemic plasma concentration [I] with $f_{u,p}$ for the hepatic interaction prediction when the $K_{i,app}$ values generated from hepatocytes plasma were utilized, the $f_{u,p}$ value was used to correct the $K_{i,app}$ for the intestinal interaction prediction because entocytes are considered as plasma protein-free environment. It is worthwhile to note that the intestinal inhibitor concentration calculated from the current model often exceeds the solubility of these drugs in intestinal fluid and generally is much higher than the $K_{i,app}$ before any $f_{u,p}$ correction ($[I]_g >> K_{i,app}$). As a result the inhibitors examined in this study are predicted to completely inhibit the CYP3A in gut wall over the time during which the victim drugs are absorbed. Therefore, the final intestinal DDI prediction depends only on the value of F_g. This point is illustrated in Figure 4b, where there is no $f_{u,p}$ correction for the $K_{i,app}$ in the intestinal interaction and the outcome of DDI prediction was similar to the performance when $f_{u,p}$ was employed. One exception to this general observation was the case of aprepitant, which displays high a $K_{i,app}$ value and a $f_{u,p}$ correction is needed for the optimal prediction of the intestinal wall DDI component.

Following initial identification of inhibitors and DDI prediction by single incubation time method, it may be desirable when examining new compounds to characterize the inhibition mechanism and estimate specific enzyme inhibition parameters. In the mechanistic approach, the incubation times with the inhibitor are 0, 10 and 20 min, and three IC_{50} curves are generated. All the data are incorporated into three models A-C (Eqs. 2-4) which are designed to differentiate reversible inhibitors, TDIs and inhibitors with both properties. These models were used to correctly indentify ketoconazole, aprepitant, fluconazole and voriconazole as reversible inhibitors; erythromycin, troleandomycin, saquinavir, clarithromycin, conivaptan, diltiazem, itraconazole and nefazodone as TDIs; ritonavir as a reversible and time dependent inhibitor. The *in vitro* inhibition constants estimated from the mechanistic models A-C were used to predict the magnitude of a DDI when combined with the total average plasma concentration of the inhibitor

and incorporated into corresponding equations. With the knowledge of inhibition mechanism, 65% of 52 clinical DDIs were accurately predicted within 2-fold of the observed fold change in AUC (Fig. 3).

The results reported here on the prediction of CYP3A DDIs using inhibitory parameters generated with human hepatocytes suspended in human plasma demonstrated that this robust system overcomes a number of perceived weaknesses associated with other *in vitro* approaches. In particular this model provides an integrated cellular environment in which all modes of hepatic metabolism are retained and the uncertainty in concentration of inhibitor at the enzyme is greatly reduced. The single incubation time method simply requires a single inhibition parameter to predict the DDI caused by CYP3A inhibition, and there is no need to correct for nonspecific binding. Furthermore, in these predictions the total average systemic plasma concentration of the inhibitor provides a reasonable value for both reversible inhibitors and TDIs without the need for the determination of fraction unbound in plasma to calculate unbound drug concentrations. The study design for inhibition using HHSHP has been simplified such that there is only one time point, no dilution step (often performed with TDIs in HLM incubation) and the same midazolam concentration (close to its K_m) is used in all IC_{50} assessments. This simple protocol design is achievable due to the fact that Model A has demonstrated the capability to extrapolate the reversible and time dependent inhibition properties simultaneously.

In summary, cryopreserved human hepatocytes suspended in human plasma were determined to be a robust and reliable system for the prediction of CYP3A DDIs. These predictions may be made by utilizing an IC_{50} determined at a single incubation time regardless of the inhibition mechanism, and if needed, mechanism may also be explored with the mechanistic method.

Acknowledgements

Thanks to Jeffrey M Weber and Shane M Lowery for the bioanalytic support.

Authorship Contribution

Participated in research design: Mao, Mohutsky, Harrelson, Wrighton and Hall

Conducted experiments: Mao, Mohutsky and Harrelson

Performed data analysis: Mao, Mohutsky and Harrelson

Wrote or contributed to the writing of the manuscript: Mao, Mohutsky, Harrelson, Wrighton and Hall

References

Ahonen J, Olkkola KT and Neuvonen PJ (1995) Effect of itraconazole and terbinafine on the pharmacokinetics and pharmacodynamics of midazolam in healthy volunteers. *Br J Clin Pharmacol* **40:**270-272.

Backman JT, Kivisto KT, Olkkola KT and Neuvonen PJ (1998) The area under the plasma concentration-time curve for oral midazolam is 400-fold larger during treatment with itraconazole than with rifampicin. *Eur J Clin Pharmacol* **54:**53-58.

Backman JT, Olkkola KT, Aranko K, Himberg JJ and Neuvonen PJ (1994) Dose of midazolam should be reduced during diltiazem and verapamil treatments. *Br J Clin Pharmacol* **37:**221-225.

Bjornsson TD, Callaghan JT, Einolf HJ, Fischer V, Gan L, Grimm S, Kao J, King SP, Miwa G, Ni L, Kumar G, McLeod J, Obach RS, Roberts S, Roe A, Shah A, Snikeris F, Sullivan JT, Tweedie D, Vega JM, Walsh J and Wrighton SA (2003a) The conduct of in vitro and in vivo drug-drug interaction studies: a Pharmaceutical Research and Manufacturers of America (PhRMA) perspective. *Drug Metab Dispos* **31:**815-832.

Bjornsson TD, Callaghan JT, Einolf HJ, Fischer V, Gan L, Grimm S, Kao J, King SP, Miwa G, Ni L, Kumar G, McLeod J, Obach SR, Roberts S, Roe A, Shah A, Snikeris F, Sullivan JT, Tweedie D, Vega JM, Walsh J and Wrighton SA (2003b) The conduct of in vitro and in vivo drug-drug interaction studies: a PhRMA perspective. *J Clin Pharmacol* **43:**443-469.

Brown HS, Chadwick A and Houston JB (2007) Use of isolated hepatocyte preparations for cytochrome P450 inhibition studies: comparison with microsomes for Ki determination. *Drug Metab Dispos* **35:**2119-2126.

Burt HJ, Galetin A and Houston JB (2010) IC_{50}-based approaches as an alternative method for assessment of time-dependent inhibition of CYP3A4. *Xenobiotica* **40:**331-343.

Chung E, Nafziger AN, Kazierad DJ and Bertino JS, Jr. (2006) Comparison of midazolam and simvastatin as cytochrome P450 3A probes. *Clin Pharmacol Ther* **79:**350-361.

Eap CB, Buclin T, Cucchia G, Zullino D, Hustert E, Bleiber G, Golay KP, Aubert AC, Baumann P, Telenti A and Kerb R (2004) Oral administration of a low dose of midazolam (75 microg) as an in vivo probe for CYP3A activity. *Eur J Clin Pharmacol* **60:**237-246.

Einolf HJ (2007) Comparison of different approaches to predict metabolic drug-drug interactions. *Xenobiotica* **37:**1257-1294.

Ernest CS, 2nd, Hall SD and Jones DR (2005) Mechanism-based inactivation of CYP3A by HIV protease inhibitors. *J Pharmacol Exp Ther* **312:**583-591.

Fahmi OA, Hurst S, Plowchalk D, Cook J, Guo F, Youdim K, Dickins M, Phipps A, Darekar A, Hyland R and Obach RS (2009) Comparison of different algorithms for predicting clinical drug-drug interactions, based on the use of CYP3A4 in vitro data: predictions of compounds as precipitants of interaction. *Drug Metab Dispos* **37:**1658-1666.

Fahmi OA, Maurer TS, Kish M, Cardenas E, Boldt S and Nettleton D (2008) A combined model for predicting CYP3A4 clinical net drug-drug interaction based on

CYP3A4 inhibition, inactivation, and induction determined in vitro. *Drug Metab Dispos* **36:**1698-1708.

Galetin A, Gertz M and Houston JB (2008) Potential role of intestinal first-pass metabolism in the prediction of drug-drug interactions. *Expert Opin Drug Metab Toxicol* **4:**909-922.

Gomez DY, Wacher VJ, Tomlanovich SJ, Hebert MF and Benet LZ (1995) The effects of ketoconazole on the intestinal metabolism and bioavailability of cyclosporine. *Clin Pharmacol Ther* **58:**15-19.

Gorski JC, Jones DR, Haehner-Daniels BD, Hamman MA, O'Mara EM, Jr. and Hall SD (1998) The contribution of intestinal and hepatic CYP3A to the interaction between midazolam and clarithromycin. *Clin Pharmacol Ther* **64:**133-143.

Greenblatt DJ, von Moltke LL, Harmatz JS, Durol AL, Daily JP, Graf JA, Mertzanis P, Hoffman JL and Shader RI (2000a) Alprazolam-ritonavir interaction: implications for product labeling. *Clin Pharmacol Ther* **67:**335-341.

Greenblatt DJ, von Moltke LL, Harmatz JS, Durol AL, Daily JP, Graf JA, Mertzanis P, Hoffman JL and Shader RI (2000b) Differential impairment of triazolam and zolpidem clearance by ritonavir. *J Acquir Immune Defic Syndr* **24:**129-136.

Greenblatt DJ, von Moltke LL, Harmatz JS, Fogelman SM, Chen G, Graf JA, Mertzanis P, Byron S, Culm KE, Granda BW, Daily JP and Shader RI (2003) Short-term exposure to low-dose ritonavir impairs clearance and enhances adverse effects of trazodone. *J Clin Pharmacol* **43:**414-422.

Grime KH, Bird J, Ferguson D and Riley RJ (2009) Mechanism-based inhibition of cytochrome P450 enzymes: an evaluation of early decision making in vitro approaches and drug-drug interaction prediction methods. *Eur J Pharm Sci* **36:**175-191.

Gurley B, Hubbard MA, Williams DK, Thaden J, Tong Y, Gentry WB, Breen P, Carrier DJ and Cheboyina S (2006) Assessing the clinical significance of botanical supplementation on human cytochrome P450 3A activity: comparison of a milk thistle and black cohosh product to rifampin and clarithromycin. *J Clin Pharmacol* **46:**201-213.

Gurley BJ, Swain A, Hubbard MA, Hartsfield F, Thaden J, Williams DK, Gentry WB and Tong Y (2008) Supplementation with goldenseal (Hydrastis canadensis), but not kava kava (Piper methysticum), inhibits human CYP3A activity in vivo. *Clin Pharmacol Ther* **83:**61-69.

Hardman JG, Limbird LE and Gilman AG (2001) Goodman & Gilman's The Pharmacological Basis of Therapeutics, 10th ed. *McGraw-Hill* **New York**.

Isoherranen N, Kunze KL, Allen KE, Nelson WL and Thummel KE (2004) Role of itraconazole metabolites in CYP3A4 inhibition. *Drug Metab Dispos* **32:**1121-1131.

Ito K, Iwatsubo T, Kanamitsu S, Ueda K, Suzuki H and Sugiyama Y (1998) Prediction of pharmacokinetic alterations caused by drug-drug interactions: metabolic interaction in the liver. *Pharmacol Rev* **50:**387-412.

Kaminsky LS and Fasco MJ (1991) Small intestinal cytochromes P450. *Crit Rev Toxicol* **21:**407-422.

Kharasch ED, Walker A, Hoffer C and Sheffels P (2004) Intravenous and oral alfentanil as in vivo probes for hepatic and first-pass cytochrome P450 3A activity:

noninvasive assessment by use of pupillary miosis. *Clin Pharmacol Ther* **76:**452-466.

Kharasch ED, Walker A, Hoffer C and Sheffels P (2005) Sensitivity of intravenous and oral alfentanil and pupillary miosis as minimally invasive and noninvasive probes for hepatic and first-pass CYP3A activity. *J Clin Pharmacol* **45:**1187-1197.

Kirby BJ and Unadkat JD (2010) Impact of ignoring extraction ratio when predicting drug-drug interactions, fraction metabolized, and intestinal first-pass contribution. *Drug Metab Dispos* **38:**1926-1933.

Kunze KL, Nelson WL, Kharasch ED, Thummel KE and Isoherranen N (2006) Stereochemical aspects of itraconazole metabolism in vitro and in vivo. *Drug Metab Dispos* **34:**583-590.

Lam YW, Alfaro CL, Ereshefsky L and Miller M (2003) Pharmacokinetic and pharmacodynamic interactions of oral midazolam with ketoconazole, fluoxetine, fluvoxamine, and nefazodone. *J Clin Pharmacol* **43:**1274-1282.

Lu C, Berg C, Prakash SR, Lee FW and Balani SK (2008a) Prediction of pharmacokinetic drug-drug interactions using human hepatocyte suspension in plasma and cytochrome P450 phenotypic data. III. In vitro-in vivo correlation with fluconazole. *Drug Metab Dispos* **36:**1261-1266.

Lu C, Hatsis P, Berg C, Lee FW and Balani SK (2008b) Prediction of pharmacokinetic drug-drug interactions using human hepatocyte suspension in plasma and cytochrome P450 phenotypic data. II. In vitro-in vivo correlation with ketoconazole. *Drug Metab Dispos* **36:**1255-1260.

Lu C, Miwa GT, Prakash SR, Gan LS and Balani SK (2007) A novel model for the prediction of drug-drug interactions in humans based on in vitro cytochrome p450 phenotypic data. *Drug Metab Dispos* **35:**79-85.

Majumdar AK, McCrea JB, Panebianco DL, Hesney M, Dru J, Constanzer M, Goldberg MR, Murphy G, Gottesdiener KM, Lines CR, Petty KJ and Blum RA (2003) Effects of aprepitant on cytochrome P450 3A4 activity using midazolam as a probe. *Clin Pharmacol Ther* **74:**150-156.

Majumdar AK, Yan KX, Selverian DV, Barlas S, Constanzer M, Dru J, McCrea JB, Ahmed T, Frick GS, Kraft WK, Petty KJ and Greenberg HE (2007) Effect of aprepitant on the pharmacokinetics of intravenous midazolam. *J Clin Pharmacol* **47:**744-750.

Mayhew BS, Jones DR and Hall SD (2000) An in vitro model for predicting in vivo inhibition of cytochrome P450 3A4 by metabolic intermediate complex formation. *Drug Metab Dispos* **28:**1031-1037.

McCrea J, Prueksaritanont T, Gertz BJ, Carides A, Gillen L, Antonello S, Brucker MJ, Miller-Stein C, Osborne B and Waldman S (1999) Concurrent administration of the erythromycin breath test (EBT) and oral midazolam as in vivo probes for CYP3A activity. *J Clin Pharmacol* **39:**1212-1220.

McGinnity DF, Berry AJ, Kenny JR, Grime K and Riley RJ (2006) Evaluation of time-dependent cytochrome P450 inhibition using cultured human hepatocytes. *Drug Metab Dispos* **34:**1291-1300.

Muirhead GJ, Wulff MB, Fielding A, Kleinermans D and Buss N (2000) Pharmacokinetic interactions between sildenafil and saquinavir/ritonavir. *Br J Clin Pharmacol* **50:**99-107.

NDA 021697. http://www.accessdata.fda.gov/scripts/cder/drugsatfda/index.cfm?fuseaction=Search.Overview&DrugName=VAPRISOL

Obach RS, Walsky RL and Venkatakrishnan K (2007) Mechanism-based inactivation of human cytochrome p450 enzymes and the prediction of drug-drug interactions. *Drug Metab Dispos* **35:**246-255.

Obach RS, Walsky RL, Venkatakrishnan K, Gaman EA, Houston JB and Tremaine LM (2006) The utility of in vitro cytochrome P450 inhibition data in the prediction of drug-drug interactions. *J Pharmacol Exp Ther* **316:**336-348.

Okudaira T, Kotegawa T, Imai H, Tsutsumi K, Nakano S and Ohashi K (2007) Effect of the treatment period with erythromycin on cytochrome P450 3A activity in humans. *J Clin Pharmacol* **47:**871-876.

Olkkola KT, Ahonen J and Neuvonen PJ (1996) The effects of the systemic antimycotics, itraconazole and fluconazole, on the pharmacokinetics and pharmacodynamics of intravenous and oral midazolam. *Anesth Analg* **82:**511-516.

Olkkola KT, Aranko K, Luurila H, Hiller A, Saarnivaara L, Himberg JJ and Neuvonen PJ (1993) A potentially hazardous interaction between erythromycin and midazolam. *Clin Pharmacol Ther* **53:**298-305.

Olkkola KT, Backman JT and Neuvonen PJ (1994) Midazolam should be avoided in patients receiving the systemic antimycotics ketoconazole or itraconazole. *Clin Pharmacol Ther* **55:**481-485.

Olkkola KT, Palkama VJ and Neuvonen PJ (1999) Ritonavir's role in reducing fentanyl clearance and prolonging its half-life. *Anesthesiology* **91:**681-685.

Paine MF and Oberlies NH (2007) Clinical relevance of the small intestine as an organ of drug elimination: drug-fruit juice interactions. *Expert Opin Drug Metab Toxicol* **3:**67-80.

Palkama VJ, Ahonen J, Neuvonen PJ and Olkkola KT (1999) Effect of saquinavir on the pharmacokinetics and pharmacodynamics of oral and intravenous midazolam. *Clin Pharmacol Ther* **66:**33-39.

Phimmasone S and Kharasch ED (2001) A pilot evaluation of alfentanil-induced miosis as a noninvasive probe for hepatic cytochrome P450 3A4 (CYP3A4) activity in humans. *Clin Pharmacol Ther* **70:**505-517.

Quinney SK, Galinsky RE, Jiyamapa-Serna VA, Chen Y, Hamman MA, Hall SD and Kimura RE (2008a) Hydroxyitraconazole, formed during intestinal first-pass metabolism of itraconazole, controls the time course of hepatic CYP3A inhibition and the bioavailability of itraconazole in rats. *Drug Metab Dispos* **36:**1097-1101.

Quinney SK, Haehner BD, Rhoades MB, Lin Z, Gorski JC and Hall SD (2008b) Interaction between midazolam and clarithromycin in the elderly. *Br J Clin Pharmacol* **65:**98-109.

Quinney SK, Zhang X, Lucksiri A, Gorski JC, Li L and Hall SD (2010) Physiologically based pharmacokinetic model of mechanism-based inhibition of CYP3A by clarithromycin. *Drug Metab Dispos* **38:**241-248.

Rostami-Hodjegan A TG (2004) ' in Silico' simulations to assess the 'in vivo' consequences of 'in vitro' metabolic drug-drug interactions. *Drug Discovery Today* **1:**441-448.

Rowland Yeo K, Jamei M, Yang J, Tucker GT and Rostami-Hodjegan A (2010) Physiologically based mechanistic modelling to predict complex drug-drug interactions involving simultaneous competitive and time-dependent enzyme inhibition by parent compound and its metabolite in both liver and gut - the effect of diltiazem on the time-course of exposure to triazolam. *Eur J Pharm Sci* **39:**298-309.

Saari TI, Laine K, Leino K, Valtonen M, Neuvonen PJ and Olkkola KT (2006) Effect of voriconazole on the pharmacokinetics and pharmacodynamics of intravenous and oral midazolam. *Clin Pharmacol Ther* **79:**362-370.

Schwenk M (1988) Mucosal biotransformation. *Toxicol Pathol* **16:**138-146.

Templeton IE, Thummel KE, Kharasch ED, Kunze KL, Hoffer C, Nelson WL and Isoherranen N (2008) Contribution of itraconazole metabolites to inhibition of CYP3A4 in vivo. *Clin Pharmacol Ther* **83:**77-85.

Tsunoda SM, Velez RL, von Moltke LL and Greenblatt DJ (1999) Differentiation of intestinal and hepatic cytochrome P450 3A activity with use of midazolam as an in vivo probe: effect of ketoconazole. *Clin Pharmacol Ther* **66:**461-471.

Wang YH (2010) Confidence assessment of the Simcyp time-based approach and a static mathematical model in predicting clinical drug-drug interactions for mechanism-based CYP3A inhibitors. *Drug Metab Dispos* **38:**1094-1104.

Wang YH, Jones DR and Hall SD (2004) Prediction of cytochrome P450 3A inhibition by verapamil enantiomers and their metabolites. *Drug Metab Dispos* **32:**259-266.

Xu L, Chen Y, Pan Y, Skiles GL and Shou M (2009) Prediction of human drug-drug interactions from time-dependent inactivation of CYP3A4 in primary hepatocytes using a population-based simulator. *Drug Metab Dispos* **37:**2330-2339.

Yeates RA, Laufen H and Zimmermann T (1996) Interaction between midazolam and clarithromycin: comparison with azithromycin. *Int J Clin Pharmacol Ther* **34:**400-405.

Zhang X, Quinney SK, Gorski JC, Jones DR and Hall SD (2009) Semiphysiologically based pharmacokinetic models for the inhibition of midazolam clearance by diltiazem and its major metabolite. *Drug Metab Dispos* **37:**1587-1597.

Zhao P, Kunze KL and Lee CA (2005) Evaluation of time-dependent inactivation of CYP3A in cryopreserved human hepatocytes. *Drug Metab Dispos* **33:**853-861.

Zimmermann T, Yeates RA, Laufen H, Scharpf F, Leitold M and Wildfeuer A (1996) Influence of the antibiotics erythromycin and azithromycin on the pharmacokinetics and pharmacodynamics of midazolam. *Arzneimittelforschung* **46:**213-217.

Figure Legends

Figure 1. Relationship between the relative CYP3A activity and inhibitor concentration. The relative CYP3A activity is determined as the rate of 1'-OH midazolam formation in the presence of inhibitor to that in the absence of inhibitor. The best fit among three models for each inhibitor was chosen and presented as following: a.) ketoconazole by Model C; b.) erythromycin by Model B; c.) itraconazole by Model B; d.) ritonavir by Model A. The closed circles represent 0 min inhibitor incubation alone, and the solid lines represent the best fits for 0 min inhibitor concentration; the closed diamonds represent 10 min inhibitor incubation alone, and the long dashed lines represent the best fits for 10 min inhibitor concentration; the closed squares represent 20 min inhibitor incubation alone, and the dotted lines represent the best fits for 20 min inhibitor concentration.

Figure 2. The single incubation time method: comparison of observed versus predicted AUC ratios. The square boxes correspond to areas of weak (1 to 2-fold increase in AUC ratio), moderate (2 to 5–fold increase in AUC ratio) and strong (> 5-fold increase in AUC ratio) inhibition. The solid line depicts the line of unity; the long dashed line represents a twofold deviation from unity; the short dashed line represents a threefold deviation from unity (13 drugs and 52 clinical DDIs).

Figure 3. The mechanistic method: comparison of observed versus predicted AUC ratios (13 drugs and 52 clinical DDIs). The square boxes correspond to areas of weak (1 to 2-fold increase in AUC ratio), moderate (2 to 5–fold increase in AUC ratio) and strong (> 5-fold increase in AUC ratio) inhibition. The solid line depicts the line of unity; the long dashed line represents a twofold deviation from unity; the short dashed line represents a threefold deviation from unity.

Figure 4. The single incubation time method: comparison of observed versus predicted AUC ratios. Panel a: The square boxes correspond to areas of weak (1 to 2-fold increase in AUC ratio), moderate (2 to 5–fold increase in AUC ratio) and strong (> 5-fold increase in AUC ratio)

inhibition. The solid line depicts the line of unity; the long dashed line represents a twofold deviation from unity; the short dashed line represents a threefold deviation from unity (12 drugs and 46 clinical DDIs). The baseline value of $F_{g,midazolam}$ used in Fig. 2 (0.57) were changed to 0.40. Panel b, $f_{u,p}$ used in Fig 2 were changed to 1 (no $f_{u,p}$ correction of $K_{i,app}$ for the intestinal interaction, 13 drugs and 52 clinical DDIs).

DMD Fast Forward. Published on January 6, 2011 as DOI: 10.1124/dmd.110.036400
This article has not been copyedited and formatted. The final version may differ from this version.

Table 1. IC_{50} values of inhibitors from human hepatocytes suspended in human plasma: single IC_{50} assessment (20 min inhibitor incubation alone) and independent multiple IC_{50} assessment (0, 10 and 20 min inhibitor incubation alone).

Inhibitor	***IC_{50} (μM)***			
	Single IC_{50} assessment	***Multiple IC_{50} assessment***		
Inhibitor incubation alone (min)	***20***	***0***	***10***	***20***
Ketoconazole	1.26 ± 0.23	0.98 ± 0.14	1.08 ± 0.11	1.14 ± 0.21
Fluconazole	7.61 ± 2.67	7.05 ± 1.83	8.05 ± 1.78	7.57 ± 2.34
Aprepitant	24.10 ± 7.30	35.62 ± 8.30	38.10 ± 10.40	23.09 ± 6.80
Voriconazole	3.01 ± 0.58	3.82 ± 0.73	4.20 ± 0.39	3.32 ± 0.64
Nefazodone	1.70 ± 0.31	27.21 ± 9.15	4.75 ± 0.93	1.59 ± 0.23
Troleandomycin	0.16 ± 0.02	3.48 ± 0.49	0.54 ± 0.11	0.23 ± 0.03
Erythromycin	2.64 ± 0.93	12.73 ± 3.02	4.79 ± 0.89	2.58 ± 0.82
Clarithromycin	1.98 ± 0.60	16.24 ± 4.11	2.55 ± 1.33	1.68 ± 0.47
Diltiazem	1.94 ± 0.24	3.83 ± 0.88	2.22 ± 0.73	2.28 ± 0.99
Saquinavir	4.57 ± 0.52	5.56 ± 1.06	7.09 ± 3.26	3.83 ± 0.64
Itraconazole	0.22 ± 0.05	0.78 ± 0.12	1.22 ± 0.15	0.37 ± 0.06
Conivaptan	1.70 ± 0.56	46.11 ± 15.97	2.69 ± 0.67	1.53 ± 0.17
Ritonavir	0.15 ± 0.01	0.16 ± 0.01	0.13 ± 0.01	0.13 ± 0.01

Note: Each number represents the mean and standard error of estimate of triplicates.

DMD Fast Forward. Published on January 6, 2011 as DOI: 10.1124/dmd.110.036400
This article has not been copyedited and formatted. The final version may differ from this version.

Table 2. Inhibition constants predicted from the best fit of models A-C.

Inhibitor	*Inhibition constant*			
	Predicted by Model*	K_i (μM)	K_I (μM)	k_{inact} (min^{-1})
Ketoconazole	C	0.59 ± 0.09		
Fluconazole	C	4.01 ± 0.62	-	-
Aprepitant	C	11.34 ± 0.72	-	-
Voriconazole	C	1.62 ± 0.13	-	-
Nefazodone	B	-	22.43 ± 7.37	0.05 ± 0.005
Troleandomycin	B	-	5.93 ± 1.32	0.07 ± 0.003
Erythromycin	B	-	25.15 ± 4.90	0.08 ± 0.005
Clarithromycin	B	-	37.43 ± 9.24	0.09 ± 0.008
Diltiazem	B	-	2.71 ± 0.73	0.04 ± 0.004
Saquinavir	B	-	4.67 ± 2.35	0.03 ± 0.005
Itraconazole	B	-	5.14 ± 1.37	0.05 ± 0.001
Conivaptan	B	-	3.26 ± 1.10	0.03 ± 0.004
Ritonavir	A	8.59 ± 3.75	0.82 ± 0.14	0.09 ± 0.01
Ritonavir	C	0.06 ± 0.01	-	-

* Three inhibition models incorporating irreversible (Model B), reversible (Model C), or both (Model A), were employed to estimate the inactivation parameters (K_I and k_{inact}) and/or reversible inhibition constant (K_i) for each inhibitor. Refer to the Methods Section for details of the models.

Table 3. Predictions of CPY3A mediated DDIs from in vitro inhibition parameters using the single incubation time method and the mechanistic method (52 clinical DDIs/13 drugs)

Inhibitor	*Inhibitor Dose* *Regimen**	*[I]*[¶] *(µM)*	$f_{u,p}$	*Victim drug*[γ]	*Predicted in AUC* *Single incubation time* [#]	*Fold increase* *Mechanistic method*[$]	*Observed fold-increase in AUC*[¥] (Mean±SD)	*Reference*
Ketoconazole	400 mg, qd, 4d, p.o.	2.82	0.01	Midazolam D4, 1h after	7.52	7.59	15.90 ± 2.90	(Olkkola et al., 1994)
Ketoconazole	400 mg, qd, 10d, p.o.	2.82	0.01	Midazolam D6	7.50	7.59	9.51	(Chung et al., 2006)
Ketoconazole	200 mg, bid, 2d, p.o.	3.46	0.01	Midazolam D1, 2nd	8.47	8.53	16.00 ± 6.1	(Tsunoda et al., 1999)
Ketoconazole	200 mg, bid, 2d, p.o	3.46	0.01	Midazolam, i.v. D1, 2nd	3.21	3.32	5.10 ± 1.90	(Tsunoda et al., 1999)
Ketoconazole	200 mg, bid, 2d, p.o.	4.76	0.01	Midazolam D2	10.07	10.16	6.47 ± 3.4	(Eap et al., 2004)
Ketoconazole	200 mg, qd, 12d, p.o.	1.88	0.01	Midazolam D12, 1h after	5.95	6.00	7.72 ± 5.96	(Lam et al., 2003)
Ketoconazole	200 mg, sd, p.o.	1.87	0.01	Midazolam 2h after	5.93	5.99	6.45	(McCrea et al., 1999)
Fluconazole	400 mg, sd, p.o.	21.55	0.89	Midazolam 2h after	8.25	7.99	3.51 ± 1.7	(Olkkola et al., 1996)
Fluconazole	D1: 400mg; D2-D5: 200 mg, qd, p.o.	29.99	0.89	Midazolam D6, 2h after	9.75	9.46	3.60 ± 2.1	(Olkkola et al., 1996)
Fluconazole	100 mg, sd, p.o.	5.6	0.89	Midazolam 1h after	3.71	3.60	2.16 ± 1.2	(Kharasch et al., 2005)

Aprepitant	125mg, sd, p.o.	1.72	0.05	Midazolam 1h after	1.96	1.86	2.27	(Majumdar et al., 2003)
Aprepitant	D1: 125mg; D2-5: 80mg, qd, p.o.	2.22	0.05	Midazolam D5, 1h after	2.02	1.90	3.30	(Majumdar et al., 2003)
Aprepitant	40mg, sd, p.o.	0.41	0.05	Midazolam 1h after	1.72	1.67	1.22	(Majumdar et al., 2003)
Aprepitant	D1: 40mg; D2-5: 25mg, qd, p.o.	0.3	0.05	Midazolam D5, 1h after	1.71	1.70	1.02	(Majumdar et al., 2003)
Aprepitant	125 mg, sd. p.o.	3.11	0.05	Midazolam, i.v 1h after	1.14	1.15	1.47 ± 0.14	(Majumdar et al., 2007)
Voriconazole	D1: 400mg; D2: 200mg, bid, p.o.	1.64	0.42	Midazolam, i.v. D2, 1h after	1.57	1.53	3.61	(Saari et al., 2006)
Voriconazole	D1: 400mg; D2: 200mg, bid, p.o.	1.46	0.42	Midazolam D2, 1h after	3.23	3.16	9.85	(Saari et al., 2006)
Nefazodone	D1-D4: 100mg titration to 200mg, bid; D5-D12: 200mg, bid, p.o.	1.73	0.01	Midazolam D12, 1h after 2nd	4.66	11.66	4.44	(Lam et al., 2003)
Troleandomycin	500 mg, bid, p.o.	1.76	0.04	Midazolam, i.v. 2h after 1st	5.83	7.20	3.02 ± 1.44	(Phimmasone and Kharasch, 2001)
Troleandomycin	500 mg, bid, p.o.	1.76	0.04	Midazolam, i.v. 2h after 1st	5.83	7.20	4.50 ± 1.0	(Kharasch et al., 2004)
Troleandomycin	500 mg, bid, p.o.	1.76	0.04	Midazolam 2h after 1st	15.88	19.79	15.70 ± 2.17	(Kharasch et al., 2004)
Erythromycin	200 mg, qid,7d, p.o.	0.44	0.16	Midazolam D7, 1h after 1st	2.37	6.87	3.38 ± 1.40	(Okudaira et al., 2007)
Erythromycin	200 mg, qid, 4d, p.o.	0.44	0.16	Midazolam D4, 1h after 1st	2.37	6.87	3.38 ± 1.60	(Okudaira et al., 2007)
Erythromycin	200 mg, qid, 2d, p.o.	0.44	0.16	Midazolam D2, 1h after 1st	2.37	6.87	2.32 ± 0.90	(Okudaira et al., 2007)

Erythromycin	500 mg, tid, 5d, p.o.	0.95	0.16	Midazolam D5, 1.5h after 1st	3.08	10.46	3.81 ± 0.70	(Zimmermann et al., 1996)
Erythromycin	500 mg, tid, 6d, p.o.	4.22	0.16	Midazolam D6, 2h after 2nd	6.47	18.05	4.41 ± 1.04	(Olkkola et al., 1993)
Erythromycin	500 mg, tid, 6d, p.o.	1.64	0.16	Midazolam, i.v. D6, 2h after 2nd	1.64	5.11	2.17± 0.38	(Olkkola et al. 1993)
Clarithromycin	500 mg, bid, 7d, p.o.	0.90	0.5	Midazolam, i.v. D7, 2h after 1st	1.50	3.51	3.10 ± 0.70	(Gorski et al., 1998)
Clarithromycin	500 mg, bid, 7d, p.o.	3.20	0.5	Midazolam, i.v. D7, 2h after 1st	2.47	5.84	3.20 ± 0.60	(Quinney et al., 2008b)
Clarithromycin	250 mg, bid, 5d, p.o.	2.4	0.5	Midazolam D5, 1.5h after 1st	5.24	14.11	3.60	(Yeates et al., 1996)
Clarithromycin	500mg, bid, 7d, p.o.	0.90	0.5	Midazolam D7, 2h after 1st	3.19	8.89	8.10 ± 2.40	(Gorski et al., 1998)
Clarithromycin	500mg, bid, 7d, p.o.	3.20	0.5	Midazolam D7, 2h after 1st	6.18	15.64	8.00 ± 2.20	(Quinney et al., 2008b)
Clarithromycin	500mg, bid, 7d, p.o.	0.90	0.5	Midazolam D7, 2h after 1st	3.19	8.89	5.75 ± 0.62	(Gurley et al., 2008)
Clarithromycin	500mg, bid, 7d, p.o.	0.90	0.5	Midazolam D7, 2h after 1st	3.19	8.89	7.79 ± 1.79	(Gurley et al., 2006)
Diltiazem	D1: 60mg, bid; D2: 60mg, tid, p.o.	0.38	0.22	Midazolam D2, 1h after 2nd	2.36	13.69	3.75 ± 0.11	(Backman et al., 1994)
Diltiazem	120mg, bid, 6d, p.o.	0.16	0.22	Midazolam, i.v. D6	1.09	3.60	1.77 ± 0.21	(Zhang et al., 2009)
Diltiazem	120mg, bid, 6d, p.o.	0.16	0.22	Midazolam D6	2.01	9.30	4.11 ± 0.46	(Zhang et al., 2009)
Saquinavir	1200mg, tid, 5d, p.o.	0.59	0.02	Midazolam, i.v. D3, 2h after 2nd	1.14	4.37	2.49	(Palkama et al., 1999)
Saquinavir	1200mg, tid, 5d, p.o.	0.59	0.02	Midazolam D3, 2h after 2nd	2.25	11.48	5.14	(Palkama et al., 1999)
Saquinavir	1200mg, tid, 7d, p.o.	1.15	0.02	Sildenafil D7	3.75	10.24	3.10	(Muirhead et al., 2000)

Itraconazole	200 mg, qd, 4d, p.o.	0.28	0.002	Midazolam D4, 1h after	5.28	10.12	10.79 ± 0.12	(Olkkola et al., 1994)
Itraconazole	200 mg, qd, 6d, p.o.	0.48	0.002	Midazolam D6, 2h after	7.21	12.94	6.60	(Olkkola et al., 1996)
Itraconazole	200 mg, qd, 6d, p.o.	0.11	0.002	Midazolam D1, 2h after	3.28	6.07	3.4	(Olkkola et al., 1996)
Itraconazole	200 mg, qd, 4d, p.o.	0.11	0.002	Midazolam D4	3.27	6.07	6.75	(Backman et al., 1998)
Itraconazole	100 mg, qd, 4d, p.o.	0.19	0.002	Midazolam D4, 2h after	4.27	8.25	5.74 ± 0.15	(Ahonen et al., 1995)
Conivaptan	40 mg, sd, p.o.	1.57	0.01	Midazolam	3.91	16.55	3.00	(NDA(021697)
Conivaptan	40 mg, sd, p.o.	1.57	0.01	Midazolam, i.v.	1.91	6.42	2.00	(NDA 021697)
Ritonavir	500mg,bid,7d, p.o.	14.09	0.02	Sildenafil D7	12.27	12.46	11	(Muirhead et al., 2000)
Ritonavir	D1: 200mg, tid; D2; 300mg, tid; D3: 300mg, qd, p.o.	11.09	0.02	Fentanyl, i.v. D2, 2h after 2nd	1.36	1.36	2.7	(Olkkola et al., 1999)
Ritonavir	200mg, bid, 2d, p.o.	1.66	0.02	Triazolam D2, 1h after 1st	9.60	11.12	20.60 ± 1.09	(Greenblatt et al., 2000b)
Ritonavir	D1: 200mg, qd; D2; 200mg, bid; D3: 200mg, qd, p.o.	2.21	0.02	Alprazolam D2, 1h after 1st	4.99	5.57	2.47 ± 0.06	(Greenblatt et al., 2000a)
Ritonavir	200mg, qd, 2d, p.o.	3.24	0.02	Trazodone D2, 1h after 1st	2.02	2.05	2.34 ± 0.17	(Greenblatt et al., 2003)

* Inhibitor dose regimen: 400 mg, qd, 10d, p.o. represents the inhibitor dosed at 400 mg, once a day for 10 consecutive days; ¶ The source of [I] is listed in the supplement data in details; ⁊ Victim drug: midazolam D12, 1h after 2nd represents at the 12th day, midazolam was orally given 1h after

the second dose of the inhibitor; [#] Single incubation time: utilizing the single IC_{50} value (20 min inhibitor incubation alone, the value listed in the first column in Table 1) with a model based on the reversible inhibition mechanism (Eq. 5) ; [$] Mechanistic method: utilizing the inhibition parameters estimated from models A-C (values listed in Table 2) with the corresponding model for a given mechanism of inhibition (Eq. 5, 7 and 8); [¥] clinically observed DDIs calculated by AUC in the presence and absence of inhibitor; i.v: intravenous

DMD Fast Forward. Published on January 6, 2011 as DOI: 10.1124/dmd.110.036400
This article has not been copyedited and formatted. The final version may differ from this version.

Figure 1.

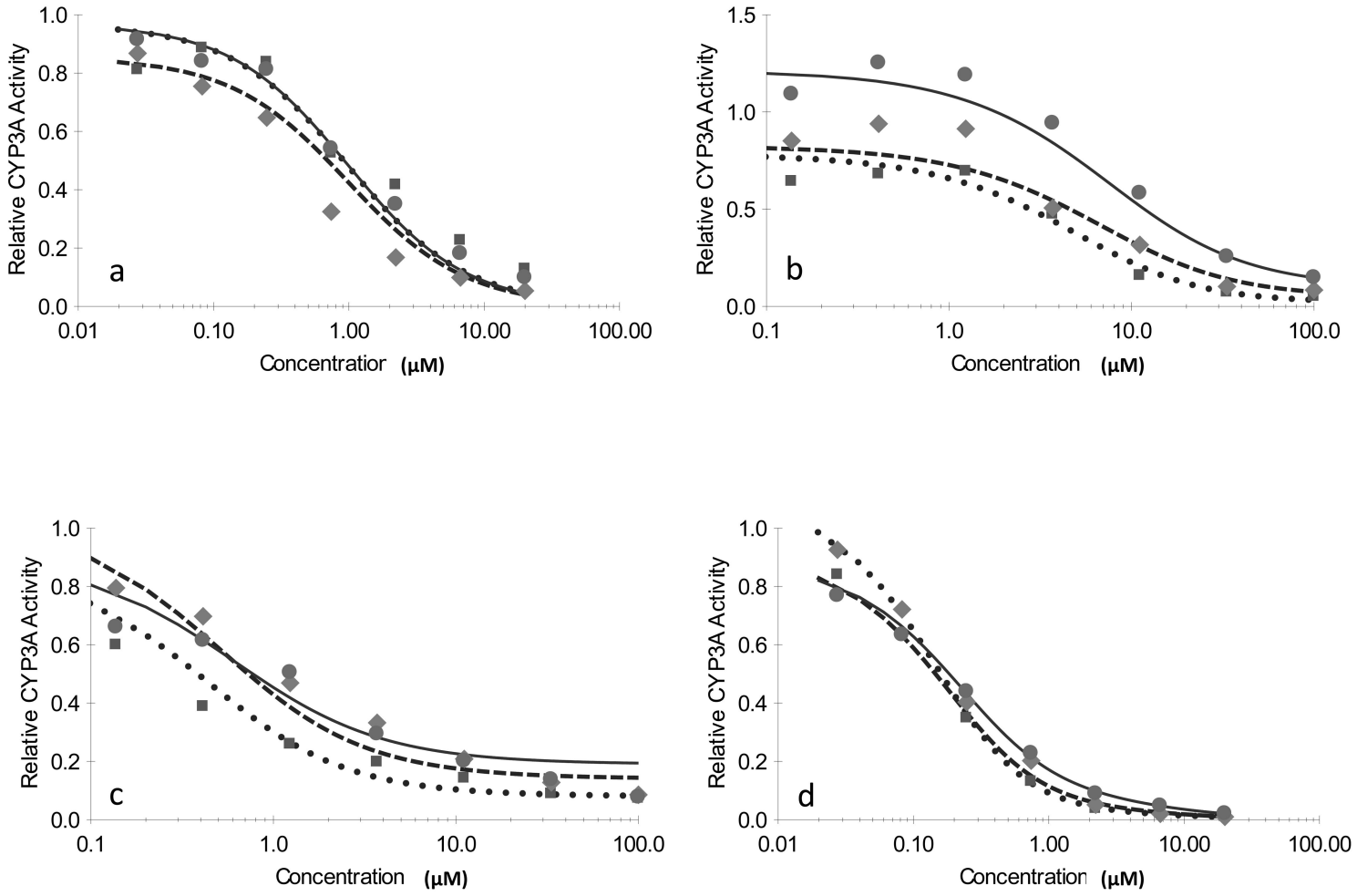

DMD Fast Forward. Published on January 6, 2011 as DOI: 10.1124/dmd.110.036400
This article has not been copyedited and formatted. The final version may differ from this version.

Figure 2.

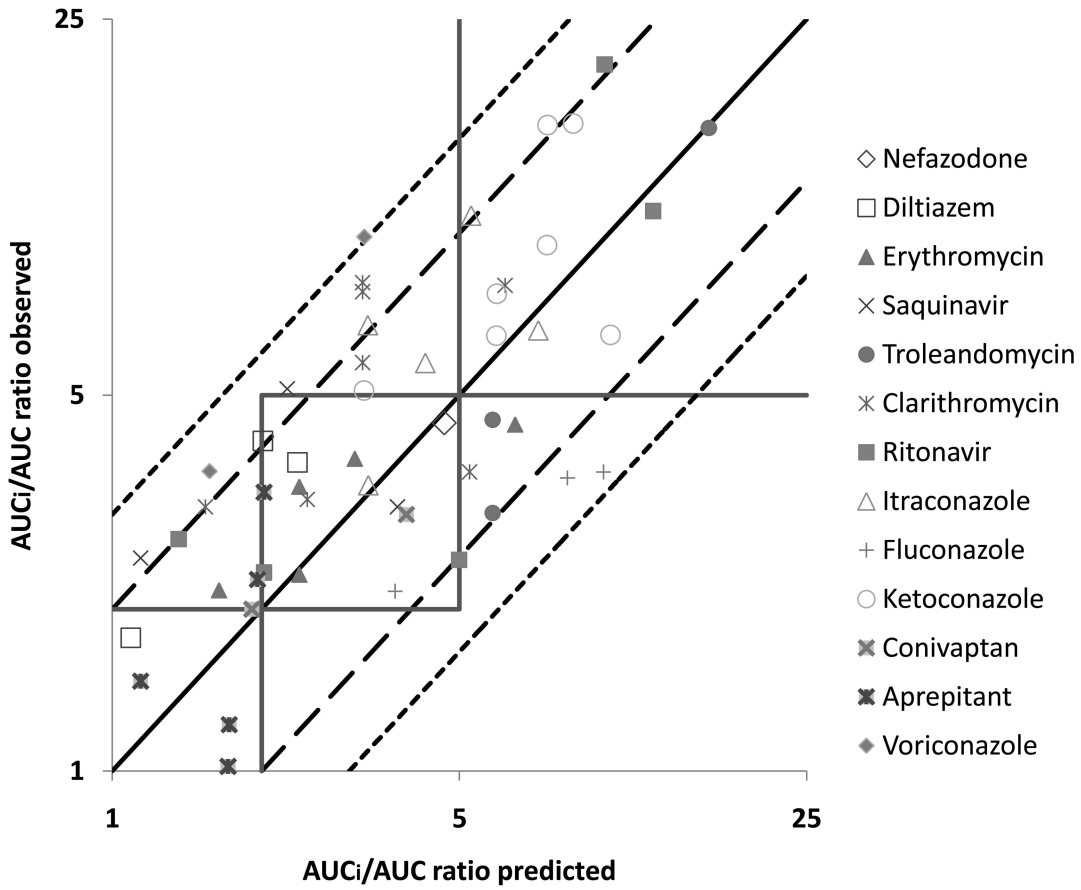

DMD Fast Forward. Published on January 6, 2011 as DOI: 10.1124/dmd.110.036400
This article has not been copyedited and formatted. The final version may differ from this version.

Figure 3.

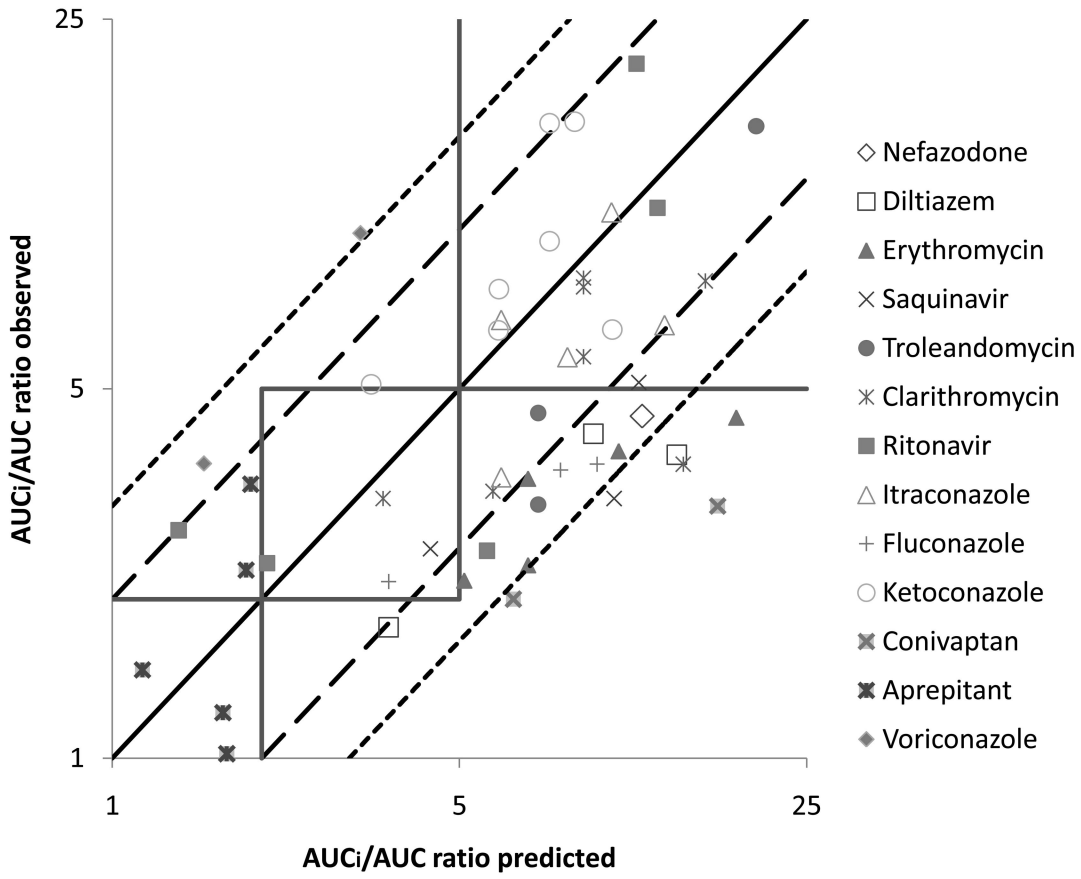

DMD Fast Forward. Published on January 6, 2011 as DOI: 10.1124/dmd.110.036400
This article has not been copyedited and formatted. The final version may differ from this version.

Figure 4.

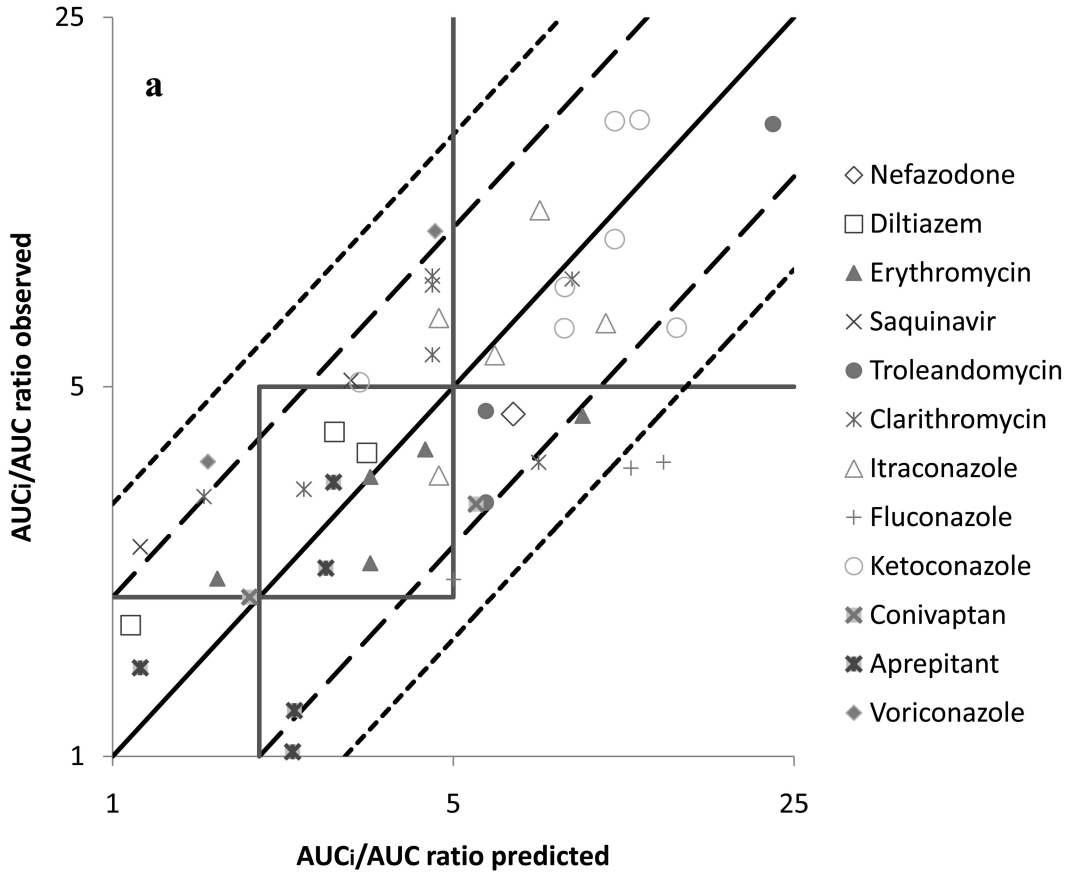

DMD Fast Forward. Published on January 6, 2011 as DOI: 10.1124/dmd.110.036400
This article has not been copyedited and formatted. The final version may differ from this version.

Figure 4.